



Study on triazophos adsorption behavior on the multi-walled carbon nanotubes

Lihong Xia^{a,†}, Lijun Luo^{a,†}, Yangmei Li^a, Tiantian Zhao^a, Wenrong Yang^b, Colin J. Barrow^b, Min Yang^{a,*}, Hongbin Wang^{a,*}

^a*School of Chemistry and Environment, Yunnan Minzu University, Kunming, Yunnan, 650500, China, Tel. +86 13629450212; emails: 325865775@qq.com, 826677468@qq.com (M. Yang), Tel. +86 13708440749; Fax: +86 0871 65910015; emails: wanghb2152@126.com, 595530820@qq.com (H.B. Wang), Tel. +86 14787817014; email: 1339953681@qq.com (L.H. Xia), Tel. +86 13629452541; email: 10501931@qq.com (L.J. Luo), Tel. +86 15812097787; email: 775667219@qq.com (Y.M. Li), Tel. +86 15887811298; email: 391914042@qq.com (T.T. Zhao)*

^b*Centre for Chemistry and Biotechnology, School of Life and Environmental Sciences, Deakin University, Waurn Ponds, VIC 3216, Australia, Tel. +613 5227 2932; email: wenrong.yang@deakin.edu.au (W. Yang), Tel. +86 087165910017; email: colin.barrow@deakin.edu.au (C.J. Barrow)*

Received 1 March 2017; Accepted 4 October 2017

ABSTRACT

A commercial multi-walled carbon nanotube (MWCNT) was selected as an adsorbent to remove triazophos, which is a representative insecticide. The MWCNT was characterized by transmission electron microscopy, Fourier transform infrared spectroscopy and Raman spectroscopy. The effect of initial pH value, ionic strength and adsorbent dosage on the adsorption capacity of triazophos was optimized. The adsorption behaviors of triazophos on MWCNT including adsorption kinetics, isotherms and thermodynamics were investigated. The results demonstrated that the adsorption kinetics belonged to the pseudo-second-order and the adsorption rate constant was up to 1.7586 g/min; correlation coefficient was above 0.997. The Freundlich model fits better than Langmuir model, and the maximum adsorption capacity was 42.02 mg/g. The adsorption of triazophos onto MWCNT was thermodynamically feasible and spontaneous.

Keywords: Multi-walled carbon nanotubes; Organophosphorus pesticides; Triazophos; Adsorption

1. Introduction

Triazophos is a universal insecticide, which shows an obvious effective control against a variety of crop pests [1]. However, the triazophos residue will cause water pollution when it enters water environment, and then ultimately cause detrimental environmental and health effects to wild animals and human beings [2–4]. Therefore, it is necessary and meaningful to remove triazophos residue from aquatic environment. To date, the wastewater treatment methods

mainly are physical methods including physical adsorption and membrane separation method, biodegradation and chemical methods [5]. Among them, physical adsorption is generally regarded as efficient and promising way to remove this type of pollutants because of low cost, easy operation and no producing secondary harmful substances. Carbon nanotubes including multi-walled carbon nanotubes (MWCNT) and single-walled carbon nanotubes have been extensively studied as highly efficient adsorbents for dyes because it has excellent mechanical properties, high

* Corresponding author.

† Authors contributed equally to this work.

Presented at the 9th International Conference on Challenges in Environmental Science & Engineering (CESE-2016), 6–10 November 2016, Kaohsiung, Taiwan, 2016.

specific surface area and high hydrophobic nature [6–11]. However, there is no report about adsorption of triazophos on MWCNT, it is necessary to investigate the adsorption of triazophos onto MWCNT.

In this work, MWCNT was selected as an adsorbent to remove triazophos in aqueous solution, the effect factors (adsorbent dosage, adsorption time, pH value and ionic strength) were optimized, and adsorption behaviors of triazophos on MWCNT including adsorption kinetics, isotherms and thermodynamics were investigated.

2. Materials and methods

2.1. Chemicals and materials

The standard triazophos pesticide (96.5%) was provided by the ministry of agriculture pesticide quality supervision and testing center; Acetonitrile, acetone, toluene, hexane and methanol were HPLC-grade; MWCNT (labeled as GYM001) were purchased from Chengdu Organic Chemicals Co. Ltd., Chinese Academy of Sciences (Chengdu, China), its physical parameters were shown in Table 1, which was activated at 105°C for 1 h before usage.

2.2. Characterization

Morphology of MWCNT was observed on transmission electron microscope (TEM; JEM-2100-200 kV). Raman spectrum was collected by a Renishaw inVia Raman microscope (UK) with excitation laser beam wavelength of 514.5 nm, measuring range was 100–3,200 cm^{-1} ; Fourier transform infrared spectra (FT-IR) were conducted on a Nicolet iS10 FT-IR Spectrometer (Thermo Fisher Scientific, Germany) using KBr pellet technique over the wave number range of 400–4,000 cm^{-1} with a resolution of 2 cm^{-1} .

2.3. Adsorption experiment

Batch experiments were designed to investigate the kinetics, isotherms and thermodynamics of triazophos adsorption onto MWCNT.

2.3.1. Adsorption experiment

The adsorption experiment process was as follows: 5.00–50.00 mg MWCNT was added into 100 mL conical flask containing 50.00 mL of triazophos aqueous solution (8.00 mg/L), the pH values were adjusted from 2.00 to 12.00 using 1.00 mol/L HCl or 1.00 mol/L NaOH. The ionic strength was adjusted by NaCl. The suspension was shook

for 60 min at 200 rpm, then centrifuged at 3,000 rpm for 5 min. 20.00 mL transparent solution was withdrawn and added into the solid phase extraction column, then 5.00 mL acetonitrile–toluene mixture solution (3:1) was added to elute the solution. The extracted solution was evaporated by water bath rotary evaporation at 35°C, then its volume was kept to 2.00 mL by adding acetone. Finally, the resultant solution was analyzed by GC-FPD.

2.3.2. Adsorption kinetics and thermodynamics experiment

12.00 mg of MWCNT were added to 100 mL flask containing 50.00 mL of different concentrations triazophos aqueous solution (1.00, 4.00 and 8.00 mg/L). The temperature of suspension was set at 298, 308 and 318 K.

2.3.3. Adsorption isotherm experiment

Adsorption isotherm experiments were carried out by mixing 12.00 mg of MWCNT with 50.00 mL triazophos solution in a 100 mL conical flask. The initial concentration of triazophos solution varied from 1.00 mg/L to 90.00 mg/L. To reach adsorption equilibrium, the sample solution was shook continuously at 200 rpm and 298 K for 1 h.

2.4. Analytical method

The concentration of triazophos was analyzed quantitatively by gas chromatography (GC), the parameters of GC was followed: the chromatographic column was DB1701 (30 m \times 250 μm \times 0.25 μm), the temperatures of inlet and analyzer were 220°C and 250°C, the initial column temperature was 100°C, kept for 6 min and then increased to 230°C at the rate of 20°C/min, further increased to 260°C at the rate of 15°C/min and kept for 8 min. The injection volume was 1 μL , nitrogen (1.81 mL/min) and hydrogen (75 mL/min) gases were used as carrier gases, the air flow rate was 100 mL/min. The standard curve of triazophos was $y = 11,928x + 55.104$ (y and x represented peak area and concentration of the triazophos, respectively), linear range was 0.005–1 mg/L and the linear correlation coefficient $R^2 = 0.9997$.

The removal rate and adsorption capacity of triazophos on the MWCNT were calculated according to the following equations:

$$(1) \text{ Removal rate (\%)} = \frac{C_0 - C_t}{C_0} \times 100\%$$

$$R (100\%) = (C_0 - C_t)/C_0 \times 100\% \quad (1)$$

where R represents removal rate of triazophos onto MWCNT (%), C_0 is initial concentration of triazophos in aqueous solution before adsorption (mg/L), C_t is residual concentration of triazophos in aqueous solution at t time.

$$(2) \text{ Adsorption quantity (mg/g)} = \frac{C_0 - C_t}{m} \times V$$

$$Q = (C_0 - C_t)/m \times V \quad (2)$$

where Q is adsorption capacity of triazophos onto MWCNT (mg/g), m is mass of MWCNT (mg), V is volume of aqueous solution of triazophos (mL).

Table 1
Physical parameters of MWCNT

Parameter	GYM001
Diameter, nm	10~30
Length, μm	5~20
Pure, wt%	>90
Ash impurities, wt%	<3.5
Specific area, m^2/g	>300

3. Results and discussion

3.1. Characterization of MWCNT

3.1.1. TEM analysis

In order to observe the surface morphology and particle size of MWCNT, the microstructure of GYM001 was analyzed by TEM and is shown in Fig. 1. It shows that the surface of the tube wall of GYM001 was relatively smooth, tubular structure, irregular, not dispersed and attached fewer impurities. The MWCNT (GYM001) were aggregated because of the existence of Van der Waals force and the presence of impurities affected the dispersion of GYM001.

3.1.2. Fourier transform infrared spectra analysis

In order to obtain the accurate molecular structure information, the FT-IR spectrum of GYM001 was recorded and is shown in Fig. 2. It shows the strong absorption peak at $3,441.18\text{ cm}^{-1}$ belonged to the stretching vibrations of -OH and intermolecular hydrogen bonding, which may be ascribed to the adsorbed H_2O on the surface of carbon nanotubes. The strong absorption peak at $1,062.41\text{ cm}^{-1}$ was the stretching vibration of C=C of carbon nanotubes skeleton. The absorption peaks at $1,441$ and $1,639\text{ cm}^{-1}$ were the stretching vibration of C-C . The absorption peak below $1,000\text{ cm}^{-1}$ may be the absorption of impurities on MWCNT [12].

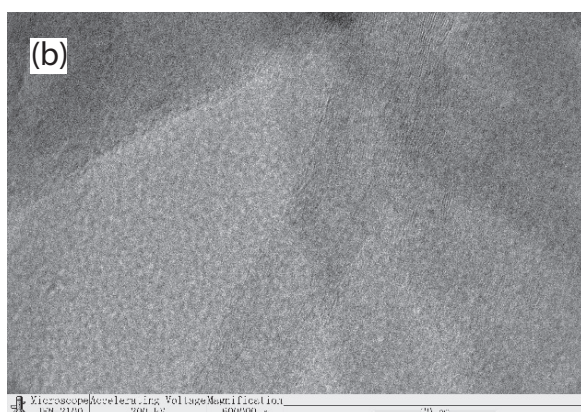
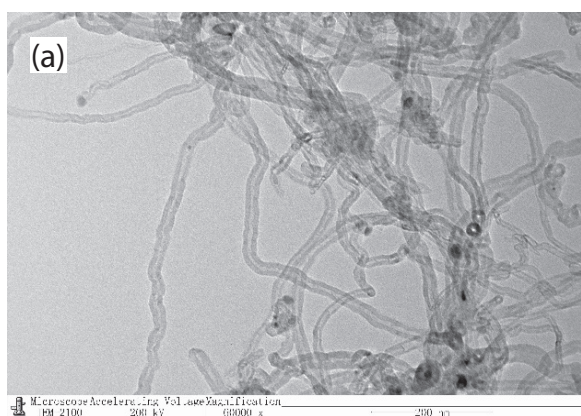


Fig. 1. TEM images of MWCNT 60000 (a) and 600000 (b).

3.1.3. Raman spectra analysis

The information of molecular vibration energy level (lattice vibration energy level) and rotational energy level structure can be obtained from Raman spectra. Fig. 3 shows the Raman spectrum of GYM001. There was the characteristic Raman peak for MWCNT at $2,600\text{ cm}^{-1}$. The peaks at $1,352$ and $1,582\text{ cm}^{-1}$ were the peaks of D and G peak. D peak reflects the degree of chaos of the structure of carbon nanotubes and G peak reaction reflects the degree of carbon nanotubes. It showed that it had defects in carbon nanotubes and the structure was disordered when the ratio (I_D/I_G) of the intensity of the two peaks was larger [13].

3.2. Effect factors on adsorption capacity of triazophos on MWCNT

3.2.1. Effect of contact time on the adsorption capacity

In order to investigate the adsorption capacity of triazophos and determine the adsorption equilibrium time, the adsorption capacity of triazophos on MWCNT (GYM001) as a function of contact time is presented in Fig. 4. The results indicated that the adsorption capacity of triazophos over

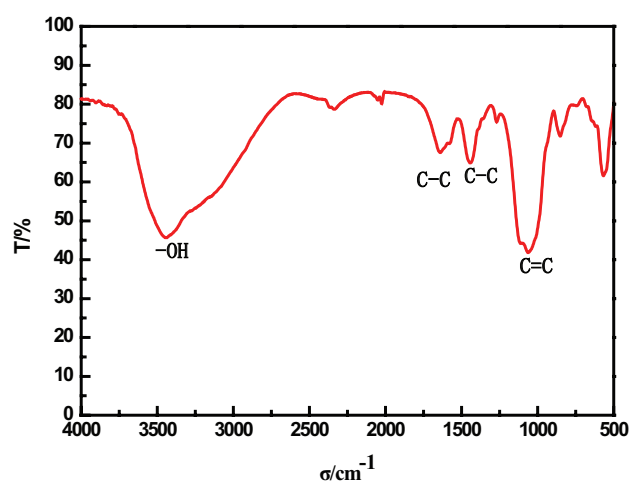


Fig. 2. FT-IR spectrum of MWCNT.

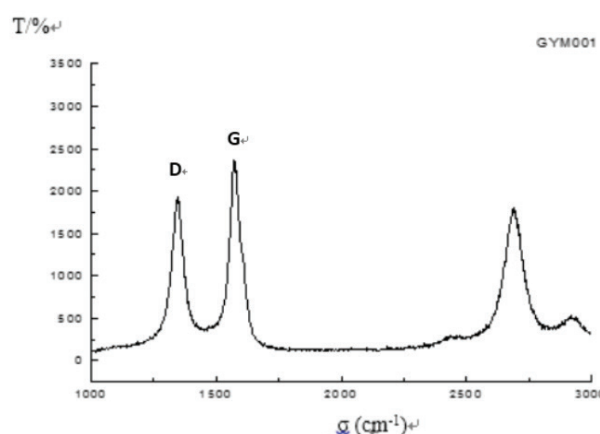


Fig. 3. Raman spectrum of MWCNT.

carbon nanotubes increased fast with the increasing of time from 0 to 20 min, and reached adsorption equilibrium less than 60 min. It maybe that the MWCNT had much more unoccupied adsorption sites in the early stages of adsorption process, and with the increasing of contact time, the more and more adsorption sites were occupied, which led to the slow adsorption rate. Therefore, the adsorption equilibrium time was selected at 60 min.

3.2.2. Effect of pH value on adsorption capacity

In order to obtain the optimal pH value, the experiment was carried out at pH 2–12 and the results are shown in Fig. 5, the adsorption capacity nearly kept unchanged (25–30 mg/g) when the pH value varied from 2 to 8. However, the adsorption capacity decreased when pH value was more than 10. The main reason maybe that triazophos is a kind of nonionic organic compound [14], pH value has a little influence on the adsorption capacity [15]. Secondary, the isoelectric point of MWCNT is 5.0, the surface of MWCNT is positively charged when the pH is less than the isoelectric point and negatively charged at high

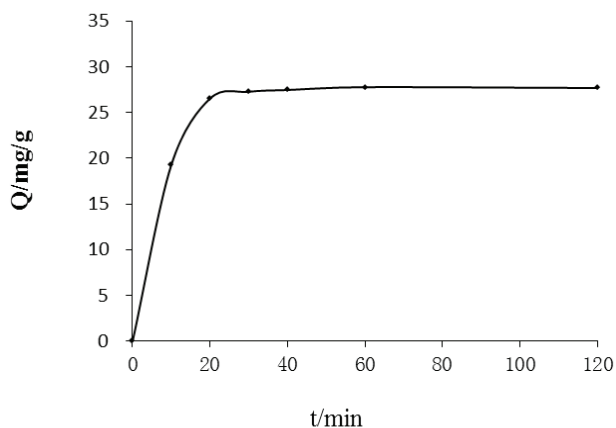


Fig. 4. Effect of contact time on adsorption capacity on MWCNT.

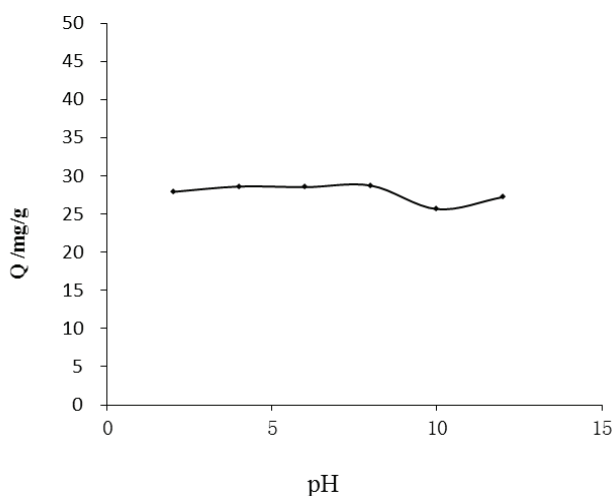


Fig. 5. Effect of pH value on adsorption capacity on MWCNT.

pH [16]. The functional groups of hydroxyl and carbonyl on the surface of MWCNT can combine with triazophos, then release H^+ , so that the measured pH value of aqueous solution was higher than the actual value under acid condition. Moreover, the hydrolysis of triazophos occurs easily in strong alkaline environment and it is stable in acidic environment [17]. Therefore, the adsorption value was not affected in acidic environment and it is caused by hydrolysis in alkaline environment. Therefore, pH value of triazophos was not adjusted because the pH value of triazophos aqueous solution was between 6 and 8.

3.2.3. Effect of adsorbent dosage on adsorption capacity

In order to obtain the optimal adsorbent dosage, the effect of adsorbent dosage on adsorption capacity was investigated and is illustrated in Fig. 6. It shows that the capacity of triazophos increased with the increase of the dosage from 0.00 to 12.00 mg, the maximum adsorption capacity reached was 29.93 mg/g. Further increasing the adsorbent dosage, the capacity decreased fast and its value reached 7.99 mg/g when the adsorbent amount was 50.00 mg. The reason was that the adsorption sites of GYM001 increased with the increasing of adsorbent dosage from 0 to 12.00, however, further increasing adsorbent dosage over 12.00 mg, there were no more adsorbate need to be adsorbed. Therefore, the adsorbent dosage was selected as 12.00 mg.

3.2.4. Effect of ionic strength on adsorption capacity

Different ionic strength may change nanoparticles agglomeration state in the process of adsorption and then affect the adsorption capacity [18]. Effect of ionic strength on adsorption capacity on MWCNT was performed and is shown in Fig. 7. The result suggested that ionic strength was not the main factor affecting the adsorption of triazophos because the adsorption capacity almost remained a constant (27 mg/g). Therefore, ionic strength was not adjusted in the following experiments.

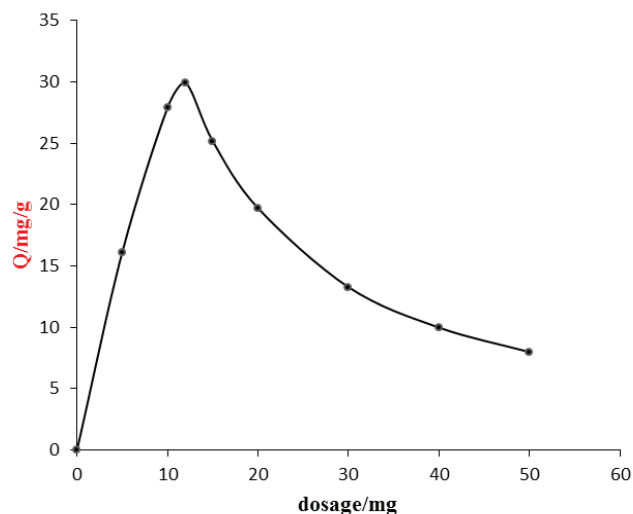


Fig. 6. Effect of adsorbent dosage on adsorption capacity on MWCNT.

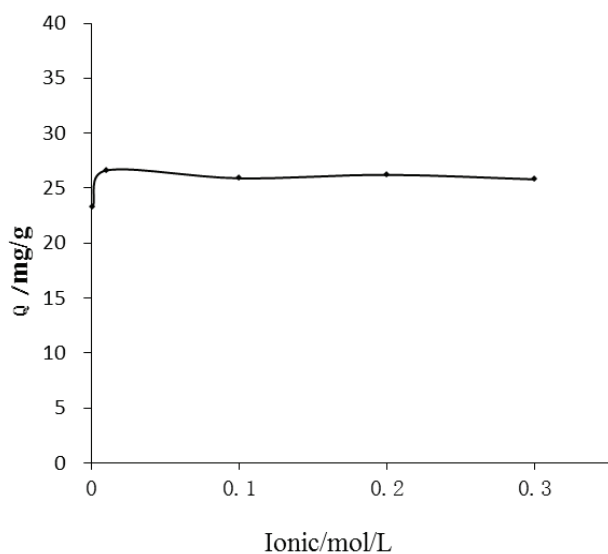


Fig. 7. Effect of ionic strength on adsorption capacity on MWCNT.

3.3. Adsorption kinetic study

The adsorption rate was an important parameter of the adsorption experiment. The pseudo-first-order rate equation assumes that the adsorption rate was determined by the number of free adsorption sites on the adsorbent surface; the pseudo-second-order kinetics model assumes that the adsorption rate was determined by the square value of the number of vacancies on the surface of the adsorbent [19]. To investigate adsorption characteristics of triazophos, adsorption processes were described by pseudo-first-order kinetic (Eq. (3)) and pseudo-second-order kinetics model (Eq. (4)) in this work:

$$\ln \frac{(q_e - q_t)}{q_e} = -\kappa_1 t \quad (3)$$

$$\frac{t}{q_t} = \frac{1}{\kappa_2 q_e^2} + \frac{1}{q_e} t \quad (4)$$

where q_e and q_t (mg/g) represent the adsorption amount of triazophos adsorbed at equilibrium and at time t , respectively. κ_1 (min^{-1}) and κ_2 ($\text{g}/(\text{mg min})$) are the pseudo-first-order and pseudo-second-order constants.

As shown in Fig. 8, at different temperatures (298, 308 and 318 K), the adsorption quantity of triazophos on carbon nanotubes were 28.25, 28.17 and 29.15 mg/g. With the increase of temperature, adsorption capacities varied from 28.17 to 29.15 mg/g. Fig. 9 presents the kinetic curves at different concentrations (1.00, 4.00 and 8.00 mg/L), the adsorption capacities were 4.02, 16.50 and 28.25 mg/g. With the increase of concentrations, adsorption capacities increased from 4.02 to 28.25 mg/g.

The above-mentioned experimental data were fitted with the pseudo-first-order and pseudo-second-order kinetics equations, and the obtained kinetic parameters are summarized in Table 2. The best-fit model was selected according to linear regression correlation coefficient (R^2)

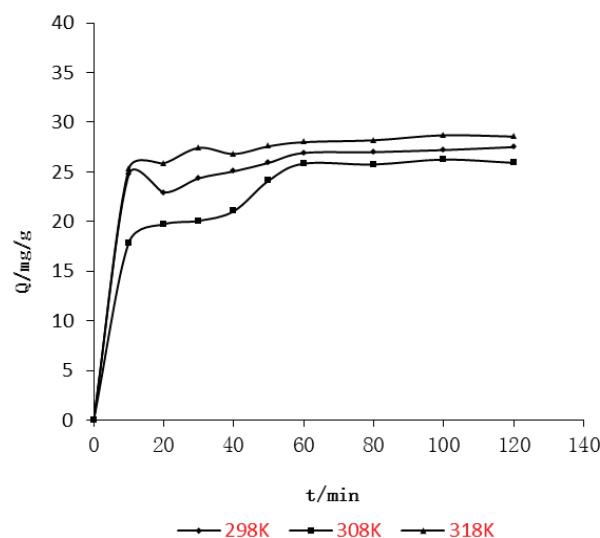


Fig. 8. The kinetic curves at different temperatures.

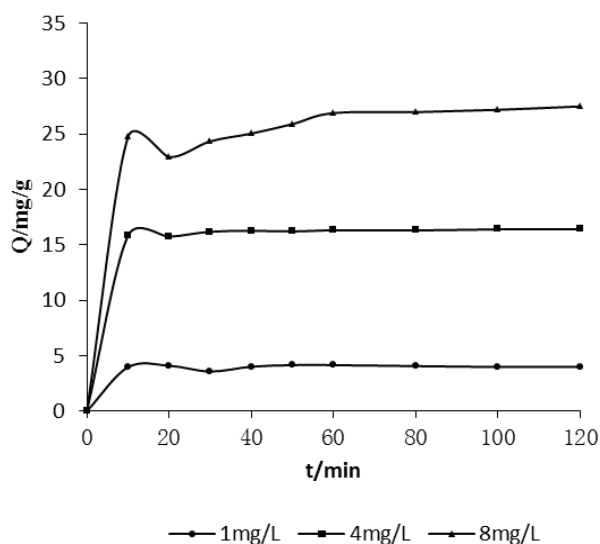


Fig. 9. The kinetic curves at different concentrations.

and theoretical Q_e (cal) value. The pseudo-second-order model for triazophos adsorption onto MWCNT can describe better than the pseudo-first-order model, because the correlation coefficients at different concentration (1.00–8.00 mg/L) and temperature (298–318 K) were above 0.99 (from 0.9972 to 1.000), the initial adsorption rate constant (h) was 28.41 $\text{mg}/(\text{g min})$, adsorption rate constant was 1.7586 $\text{mg}/(\text{g min})$, whereas the correlation coefficients of pseudo-first-order model were below 0.98 (from 0.1786 to 0.9785), adsorption rate constant was 0.0478 $\text{mg}/(\text{g min})$. The q_e (cal) values obtained from pseudo-second-order model were closer to the experimental q_e (exp) value than those obtained from pseudo-first-order model. Therefore, the adsorption behavior of triazophos adsorption onto MWCNT belonged to the pseudo-second-order kinetic model. This result implied that the adsorption process may be controlled by chemical adsorption between MWCNT.

Table 2
The obtained kinetic parameters

Variable		Actual value	First-order kinetics equation			Second-order kinetics equation			
		Q_e (mg/g)	Q_e (mg/g)	κ_1/min^{-1}	R^2	Q_e (mg/g)	h (mg/g/min)	κ_2 mg/(g/min)	R^2
C_0 (mg/L)	1	4.15	8.44	0.0125	0.1786	4.02	28.41	1.7586	0.9990
	4	16.42	1.40	0.0276	0.8799	16.50	24.21	0.0889	1.0000
	8	27.50	6.27	0.0309	0.9422	28.25	7.33	0.0092	0.9995
Temperature (K)	298	27.50	27.20	0.0420	0.9785	28.25	7.33	0.0092	0.9995
	308	26.25	25.41	0.0478	0.9127	28.17	3.18	0.0040	0.9972
	318	28.69	10.58	0.0278	0.9512	29.15	12.38	0.0146	0.9998

3.4. Adsorption isotherm study

To understand the adsorbate–adsorbent interactions, we investigated the adsorption isotherms of triazophos on MWCNT. The commonly used two equilibrium adsorption models are Langmuir adsorption model and Freundlich model. The Langmuir model was an ideal adsorption model and suitable for single component gas or liquid adsorption [20]. The Freundlich model was the empirical formula and was mainly used to describe the non-uniform surface adsorption [21]. In this work, the experimental data was fitted by Langmuir isothermal adsorption equation (Eq. (5)) and Freundlich isothermal adsorption equation (Eq. (6)):

$$\frac{1}{Q_e} = \frac{1}{K_L Q_m} \cdot \frac{1}{C_e} + \frac{1}{Q_m} \quad (5)$$

where Q_m is saturated adsorption capacity (mg/g); K_L is Langmuir adsorption equilibrium constant related to the temperature (L/mg), C_e is equilibrium concentration (mg/L).

$$\ln Q_e = \frac{1}{n} \ln C_e + \ln K_f \quad (6)$$

where Q_e is the equilibrium adsorption capacity (mg/g), n is the empirical constant related to temperature, K_f is the Freundlich adsorption equilibrium constant that could reflect the size of the adsorbent–adsorption affinity. It could show that the adsorption reaction was probable to happen easily when $1/n$ is between 0.1 and 0.5, the reaction was difficult when the $1/n$ was more than 0.5 [22].

The adsorption isotherm parameters calculated from Langmuir model and Freundlich model are listed in Table 3. The best-fit model was selected according to linear regression correlation coefficient (R^2). The Freundlich model for triazophos adsorption onto MWCNT can describe better than the Langmuir model, because the correlation coefficients at different temperature (298–318 K) for Freundlich model were above 0.95 (from 0.9597 to 0.9728), whereas the correlation coefficients of Langmuir model were below 0.89 (from 0.8555 to 0.8893). Adsorption of triazophos onto MWCNT belonged to multi-molecular layer adsorption and was much more likely because $1/n$ was greater than 0.1 and less than 0.5 (between 0.1437 and 0.1834).

Table 3
Adsorption isotherm model and related fitting parameters

T (K)	Langmuir equation			Freundlich equation		
	Q_{\max} (mg/g)	K_L (L/mg)	R^2	$1/n$	K_f	R^2
298	39.68	7.20	0.8893	0.1437	26.23	0.9742
308	42.02	1.00	0.8555	0.1652	26.47	0.9597
318	39.37	1.00	0.8883	0.1834	22.54	0.9823

3.5. Adsorption thermodynamics study

Thermodynamics function included the variable of Gibbs free energy (ΔG), enthalpy (ΔH), entropy change (ΔS), which can describe the adsorption process of direction and degree. ΔG can be used to judge the type of adsorption, the range of value of ΔG can define physical adsorption (–20 to –0 kJ/mol) or chemical adsorption (–400 to –80 kJ/mol) according to ΔG value.

$$\Delta G = -RT \ln K_c \quad (7)$$

$$K_c = \frac{C_s}{C_e} \quad (8)$$

$$\Delta G = \Delta H - T\Delta S \quad (9)$$

where T is the temperature of adsorption (K), R is gas equilibrium constant (8.314 J/(mol K)), K_c is equilibrium constant, C_s is solid concentration (mg/L), C_e is liquid phase equilibrium concentration (mg/L).

Thermodynamic function parameters were calculated. They are summarized in Table 4. ΔH and ΔS were found to be 8.17–38.44 kJ/mol and 0.11–0.35 kJ/(mol·K), which indicated that the adsorption process was endothermic and increasing disorder degree. ΔG values calculated at different concentration of triazophos were all below –24.50 kJ/mol (–24.50 to –34.76 kJ/mol), which indicated that adsorption process was thermodynamically feasible and spontaneous when the temperature varied from 298 to 318 K. Moreover, ΔG values below –24.50 kJ/mol indicated that adsorption process was chemical adsorption, and it was beneficial to the occurrence of adsorption reaction raising the temperature.

Table 4
Thermodynamic parameters

C_0 (mg/L)	T (K)	ΔG (kJ/mol)	ΔH (kJ/mol)	ΔS (kJ/mol)
1	298	-27.73	38.44	0.35
	308	-34.76		
	318	-34.48		
4	298	-28.26	6.95	0.12
	308	-29.89		
	318	-30.62		
8	298	-24.50	8.17	0.11
	308	-25.14		
	318	-26.71		

4. Conclusion

In conclusion, the structural characteristic of a commercial MWCNT and its adsorption property for triazophos were investigated. The adsorption behaviors (adsorption kinetics, isotherms and thermodynamics) of triazophos over MWCNT were investigated in detail, and the operation factors on adsorption capacity of triazophos on MWCNT were also optimized. The results indicated adsorption of triazophos on MWCNT belonged to the pseudo-second-order model and the Freundlich model, and adsorption process was thermodynamically feasible and spontaneous. It was feasible and meaningful to use MWCNT to remove hazardous insecticides such as triazophos.

Acknowledgments

This work was financially supported by National Natural Scientific Fund (No. 21767030), YMU-DEAKIN International Associated Laboratory on Functional Materials, Key Laboratory of Resource Clean Conversion in Ethnic Region, Education Department of Yunnan Province (117-02001001002107) and Natural Science Foundation of Yunnan Province (2016FB014).

References

- [1] M.J. Qu, Z.J. Han, X.J. Xu, L.N. Yue, Triazophos resistance mechanisms in the rice stem borer (*Chilo suppressalis* Walker), *Pestic. Biochem. Physiol.*, 77 (2013) 99–105.
- [2] H. Peter, S. Wood, Drivers of change in global agriculture, *Philos. Trans. R. Soc. London, Ser. B*, 363 (2008) 495–515.
- [3] B.Y. Chen, S.Y. Zhen, X.C. Niu, J.S. Zhao, Species sensitive distribution for aquatic biota exposed to triazophos, *J. Environ. Sci.*, 32 (2011) 1101–1107.
- [4] K.J. Ju, J.X. Feng, J.J. Feng, Q.L. Zhang, T.Q. Xu, J. Wei, A.J. Wang, Biosensor for pesticide triazophos based on its inhibition of acetylcholinesterase and using a glassy carbon electrode modified with coral-like gold nanostructure supported on reduced graphene oxide, *Microchim. Acta*, 182 (2015) 2427–2434.
- [5] C. Namasivayam, R.T. Yamuna, D.J.S.E. Arasi, Removal of acid violet from wastewater by adsorption on waste red mud, *Environ. Geol.*, 41 (2001) 269–273.
- [6] P.K. Kanaujia, D. Pardasani, A.K. Purohit, V. Tank, D.K. Dubey, Polyelectrolyte functionalized multi-walled carbon nanotubes as strong anion-exchange material for the extraction of acidic degradation products of nerve agents, *J. Chromatogr. A*, 1218 (2011) 9307.
- [7] R.W. Gillham, S.F. O'Hannesin, Enhanced degradation of halogenated aliphatics by zero-valent iron, *Ground Water*, 32 (1994) 958–967.
- [8] K.V. Schoutteten, T. Hennebel, E. Dheere, Effect of oxidation and catalytic reduction of trace organic contaminants on their activated carbon adsorption, *Chemosphere*, 165 (2016) 191–201.
- [9] O.G. Apul, Q. Wang, Y. Zhou, T. Karanfil, Adsorption of aromatic organic contaminants by graphene nanosheets: comparison with carbon nanotubes and activated carbon, *Water Res.*, 47 (2013) 1648–1654.
- [10] M. Kim, K.J. Wan, Purification of aromatic hydrocarbons using Ag–multiwall carbon nanotube–ZnO nanocomposites with high performance, *J. Ind. Eng. Chem.*, 47 (2016) 94–101.
- [11] C. Lu, Y.L. Chung, K.F. Chang, Adsorption of trihalomethanes from water with carbon nanotubes, *Water Res.*, 39 (2005) 1183–1189.
- [12] V. Sabna, S.G. Thampi, S. Chandrakaran, Adsorption of crystal violet onto functionalised multi-walled carbon nanotubes: equilibrium and kinetic studies, *Ecotoxicol. Environ. Saf.*, 134 (2015) 390–397.
- [13] J.X. Wu, H. Xu, J. Zhang, Raman spectroscopy of graphene, *J. Chin. Chem. Soc.*, 72 (2014) 301–318.
- [14] L.J. Zhu, W. Zhang, J.C. Zhang, D.X. Zai, R. Zhao, Thermodynamics adsorption and its influencing factors of chlorpyrifos and triazophos on the bentonite and humus, *J. Environ. Sci.*, 31 (2010) 2699–2704.
- [15] S.J. Zhang, T. Shao, S.S.K. Bekaroglu, T.J. Karanfil, Adsorption of synthetic organic chemicals by carbon nanotubes: effects of background solution chemistry, *Water Res.*, 44 (2010) 2067.
- [16] C.Y. Cui, Q.Z. Zheng, W.F. Yang, Adsorption properties of Cr³⁺ on multiwall carbon nanotubes modified by different chemical methods, *J. Environ. Eng.*, 6 (2012) 3975–3980.
- [17] T. Aungpradit, P. Sutthivaiyakit, D. Martens, S. Sutthivaiyakit, A.A. Ketrup, Photocatalytic degradation of triazophos in aqueous titanium dioxide suspension: identification of intermediates and degradation pathways, *J. Hazard. Mater.*, 146 (2007) 204–213.
- [18] J. Lee, S. Jeong, Y. Ye, V. Chen, S. Vigneswaran, Protein fouling in carbon nanotubes enhanced ultrafiltration membrane: fouling mechanism as a function of pH and ionic strength, *Sep. Purif. Technol.*, 176 (2017) 323–334.
- [19] G. Vakili-Nezhaad, M. Al-Wadhahi, A.M. Gujrathi, R. Al-Maamari, M. Mohammadi, Effect of temperature and diameter of narrow single-walled carbon nanotubes on the viscosity of nanofluid: a molecular dynamics study, *Fluid Phase Equilib.*, 434 (2017) 193–199.
- [20] G. Gürboğa, H. Tel, Preparation of TiO₂-SiO₂ mixed gel spheres for strontium adsorption, *J. Hazard. Mater.*, 120 (2005) 135.
- [21] H.Y. Gao, Z.Z. Song, W.J. Zhang, X.F. Yang, X. Wang, D.S. Wang, Synthesis of highly effective adsorbents with waste quenching blast furnace slag to remove Methyl Orange from aqueous solution, *J. Environ. Sci.*, 53 (2017) 68–77.
- [22] J. Yu, F.C. Yang, W.N. Hung, C.L. Liu, M. Yang, T.F. Lin, Prediction of powdered activated carbon doses for 2-MIB removal in drinking water treatment using a simplified HSDM approach, *Chemosphere*, 156 (2016) 374–382.